

Bending of third generation steel: Experimental and numerical approach

ESPANHOL PEREIRA Catarina Sofia^{1,2,a}, VINCZE Gabriela^{1,2,b*},
DIAS PRATES Pedro André^{1,2,c} and BUTUC Marilena Carmen^{1,2,d}

¹Centre of Mechanical Technology and Automation (TEMA), Department of Mechanical Engineering, University of Aveiro, Portugal

²LASI – Intelligent Systems Associate Laboratory, Portugal

^acsep@ua.pt, ^bgvincze@ua.pt, ^cprates@ua.pt, ^dcbutuc@ua.pt

Keywords: Bending, Advanced High-Strength Steel, Springback/Forward

Abstract. The development of a new class of material, such as third-generation advanced high-strength steel, requires a deep understanding of mechanical behaviour before its use in industry. One of the critical issues in sheet metal forming processes is dimensional accuracy, which is strongly dependent on the elastic recovery that can manifest itself as springback or spring forward [1]. This undesired defect results from the materials parameters and/or tools geometries [2]. One common way to evaluate the springback/forward is through bending tests. This work aims to investigate the existence of springback/forward on the selected material, its magnitude and dependence on the tool geometry and test the performance of the commercial finite element software Abaqus 2017 to predict the observed behaviour. The 3rd GEN steel, CR980XG3™ produced by US Steel is subjected to V-bending to evaluate the existence of springback or spring-forward. Furthermore, to evaluate the dependence of springback/forward on the tool's geometry, the V-bending tools with different bending angles (namely, 60° and 90°) and different punch radii (namely, 5° and 10°) are used. The load is applied by a Shimadzu AG-X plus 100kN, and the deformation is measured by digital image correlation (DIC) using the GOM ARAMIS 3D 5M system. Numerical analysis of the bending tests is made using Abaqus 2017 software. The experimental results show that the material exhibits springback and spring forward depending on the tool geometry. The strain distribution through the thickness is correlated with the springback/forward.

Introduction

The automotive industry has increased the production of lightweight and safe materials for vehicle components such as the body shell, brakes, steering system, and others [3]. High-tensile strength sheet metals are engineered to enhance component strength and reduce weight by creating a robust metallic structure with minimal thickness [4]. Since the new European regulations on CO2 emission, lightweight materials such as advanced high-strength steels (AHSS) are much valorised, given the vehicle's weight reduction [5]. There are three AHSS generations and this classification is based on ductility and strength [6,7]. The 3rd generation combines the low-cost and easy production of the 1st generation and the high strength and elongation of the 2nd. It also has the additional goal of minimizing the industry's environmental footprint, given the automotive production's emissions and the vehicle's fuel consumption [6,7].

In sheet metal forming processes, the V-bending process is commonly used in the industry [2,8,9], and springback often occurs, since in the bending process, the metal elasticity limit can be exceeded [3,10]. Springback results in a modification of the part's shape, posing challenges to the accuracy of the dimensions and quality of the bent components [1,11]. The change in geometry is due to elastic recovery in the sheet metal after the unloading [2,8]. In the bending process, tensile

and compressive stress occurs in the outside (pressed against the die) and inside (pressed against the punch) surfaces of the bend, respectively [11–13]. Therefore, the inner surface of the metal sheet tends to contract, while the outer side has a propensity to expand, resulting in the occurrence of springback [11,13]. Based on the bend angle achieved after the unloading, springback is called positive if this angle surpasses the final bending angle before the punch removal. In the opposite situation, springback can be called negative or spring forward [11,13]. Springback's value can be obtained through the difference between the abovementioned angles.

Several factors influence the springback occurrence in sheet metal, mainly sheet metal geometrical and mechanical properties, tools' geometrical properties, and the bending process characteristics. The goal of the present study is to investigate the existence of springback in the 3rd generation steel CR980XG3TM, its magnitude and the tool geometry influence, through bending tests. Furthermore, the Abaqus 2017 software is used to predict the springback phenomenon in the same bending conditions. Experimental and numerical studies (using the finite element method) were conducted to evaluate springback's influencing factors. Lems [14] examined the elastic constants during plastic deformation and demonstrated they suffer alteration throughout the process. Cleveland and Gosh's [15] research indicates a reduction in Young's modulus as plastic strain increases. Using the Abaqus 2017 software, Fu [16] performed a study on springback factors in air-bending tests. Fei and Hodgson [17] studied the influence of the material's (TRIP steels) mechanical properties on springback and revealed the friction's influence on the springback phenomenon. Ramezani et al. [18] also designed a model using finite element modelling to establish a relationship between springback and kinetic friction during V-bending tests, for ultra-high-tensile-strength steels. With the aid of an analytical model, and very much like the present study, Leu and Zhuang [19] studied the correlation between several factors, such as punch radius, and sheet metal thickness with the springback phenomenon in a high-strength material, through experimental tests and numerical simulation. On a more experimental procedure, Garcia-Romeu et al. [20] conducted a study with aluminium and stainless steel, concluding that an increase in die width and the bending angle increases springback in the metal sheet.

As previously noted, the present study assesses the occurrence, extent, and contributing factors of springback in third-generation steel. This objective is achieved through an experimental procedure involving bending tests and numerical simulations conducted using the Abaqus 2017 software. The use of these computational tools offers several advantages, both from an economic and ecological standpoint (eliminating the need for material acquisition, cutting, machining, and measurement) and in terms of time efficiency (negating the necessity for machinery calibration or setup, as well as the acquisition or fabrication of the bending tools).

Experimental procedure

The experimental procedure was carried out to study the springback in material USS CR980XG3TM steel. Its mechanical properties were determined in another study and the data is available in the article of Santos et al. [21]. The material exhibits a Young's modulus (E) of 195 ± 5 GPa and a Poisson's ratio (ν) of 0.289 ± 0.003 . Fig. 1 presents the material's true stress-strain curves in rolling direction (RD).

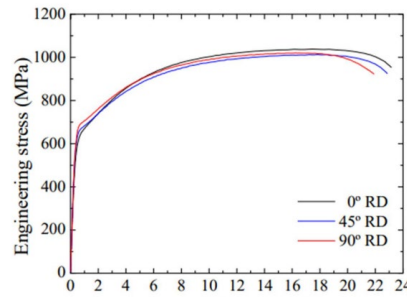


Fig. 1 - True stress-strain curves of the studied material.

The specimens' dimensions consist of 160×20×1.6 mm (approx.), obtained using a CNC machining centre. V-shaped bending tools featuring different radii and bend angles were employed. It was determined that four tests would be carried out for each bending tool. Four V-shaped punches were used, with a 60° or 90° punch angle, and a 5 or 10 mm bending radius. The tests performed with each punch and the determined displacement for each type are indicated in Table 1, along with the corresponding test specimens' thickness.

Table 1 - Punches' displacement and test specimen's average thickness.

Test	Punch displacement [mm]	Test specimen's thickness [mm]
V-P60R10	46,65	≅1,57
V-P60R5	51,75	≅1,57
V-P90R10	50,0	≅1,56
V-P90R5	52,0	≅1,56

The Shimadzu AG-X plus testing machine, controlled by the TRAPEZIUM X software, performed the bending tests, and the GOM ARAMIS 3D 5M system measure the deformation through the thickness by Digital Image Correlation (DIC) using the Aramis software. Fig. 2 exhibits the bending tests' setup.



Fig. 2 - Shimadzu and GOM ARAMIS setup, with die, punch, and test specimen in place

Strain calculations along a chosen area were conducted using the “épsilon X” option in the Aramis software. Subsequently, images capturing the maximum flexion and punch withdrawal of the specimen were saved for later springback assessment, using the SOLIDWORKS software, as observed in Fig. 3. The TRAPEZIUM software oversees the bending test. It provides information,

including force and displacement data. These values are essential for analyzing the material and tool behavior, and for visualizing force vs. displacement curves.

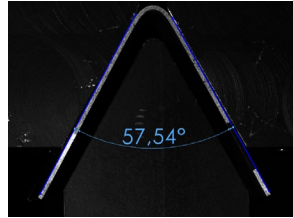


Fig. 3 - Angle measurement in SOLIDWORKS, with pictures taken by the Aramis software.

Results

Springback is estimated through angle measurements using the SOLIDWORKS software. Two images taken by the Aramis system, the first taken in the moment of maximum flexion and the second in the unloading moment, are loaded in SOLIDWORKS for angle measurement, as represented in Fig. 3. Fig. 4 illustrates the obtained mean springback value, in percentage, in the test specimens. Springback is calculated through the subtraction of the final angle value to the angle in the moment of maximum flexion, which is the following:
$$\text{springback} (\%) = \frac{\theta_d - \theta_{maxFlex}}{\theta_{maxFlex}} * 100.$$
 θ_d represents the angle after the unloading moment and $\theta_{maxFlex}$ represents the angle in the moment of maximum flexion.

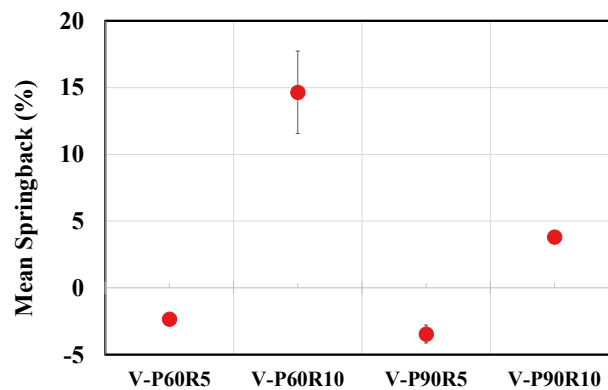


Fig. 4 - Springback results (%) in V-bending tests: P60 and P90 refer to the punch bending angle, and R5 and R10 refer to the punch radius.

The data analysis indicates that specimens subjected to punches with a smaller bending radius (5 mm) experienced less springback than those subjected to punches with a larger radius (10 mm). This behaviour is in agreement to the literature [22–24], namely: a lower bending radius causes a reduction in the specimen’s springback when compared to a higher radius. The lowest springback mean value was achieved by specimens subjected to the V-P60R5 punch, with a mean value of -2.34%; the V-P60R10 punch was responsible for causing greater springback in the specimens. It is noteworthy that punches with a smaller bending radius of 5 mm caused negative springback, i.e., spring-forward, whereas punches with a larger radius caused positive springback values.

In addition to springback analysis, it was decided to study the specimens’ strain after the bending tests. The procedure involves analyzing the images captured by the Aramis system, represented in Fig. 5, where a color gradient indicates the strain in that area. The outermost zone is marked in red, representing positive strain; the inner zone in blue represents negative strain. In between, the deformation has a neutral value, represented in green (neutral zone).

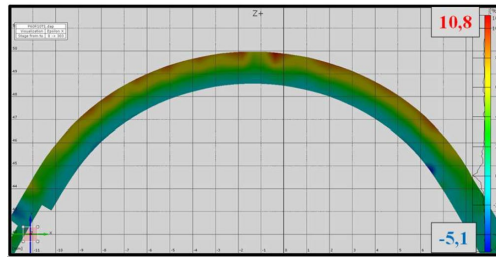


Fig. 5 - Strain distribution through the thickness observed in specimen tested with the V-P60R10 punch (image from Aramis); the red value (10,8%) is the maximum strain value and the blue value (-5,1%) is the lowest.

For each punch, the mean of both the maximum positive and negative deformation values was computed across all specimens subjected to that specific punch. The results are illustrated in Fig. 6.

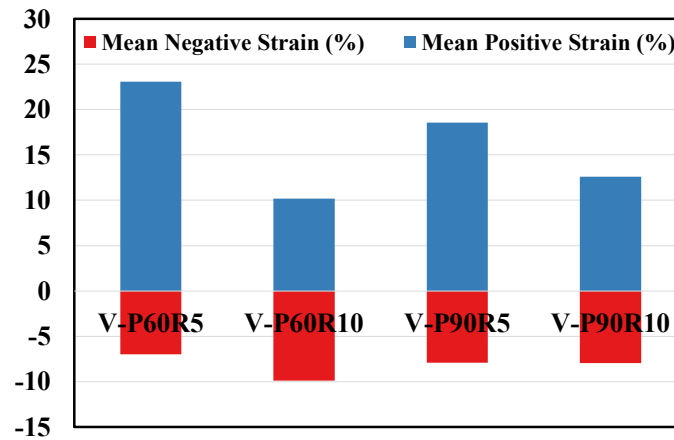


Fig. 6 - Mean strain in the test specimens.

Concerning the average positive strain, the V-P60R5 punch achieved the highest value, registering 23.07% of strain. Subsequently, the V-P90R5 punch followed with an average positive strain of 18.55%. In contrast, the V-P60R10 punch exhibited the lowest mean positive strain at 10.18%. The 5 mm radius punches induced a greater positive strain in the test specimens when compared with the 10 mm radius punches. This behaviour agrees with the literature [22–24]. The V-P60R10 punch yielded the highest mean negative strain at -9.89%, while the remaining punches exhibited comparable negative strain values. A relationship can be established between springback and strain, as specimens subjected to punches with smaller bending radii exhibit less springback and higher strain. The opposite is observed in specimens subjected to the 10 mm radius punch. It is noted that the occurrence of spring-forward is consistent with the use of the 5 mm bending radius, which may be related to a higher positive strain value.

The analysis of the maximum force exerted for each test specimen follows, where the data were recorded by the TRAPEZIUM software and are illustrated in Fig. 7.

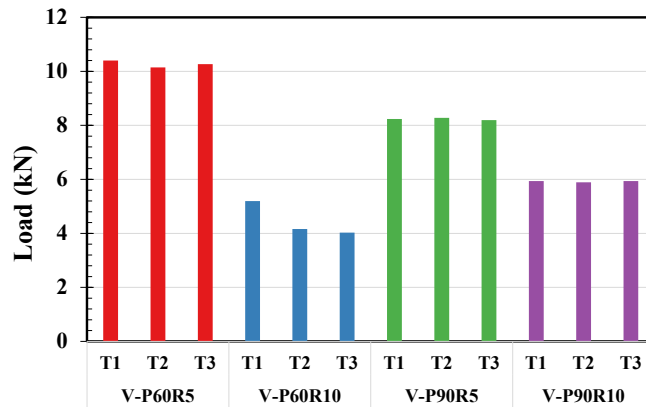


Fig. 7 - Maximum load applied in the test specimens in each punch.

Examining the results, it is observed that the test specimens subjected to the 5 mm radius punches experienced a higher maximum load when compared to those subjected to the remaining punches. The highest and lowest values of the maximum load were achieved by the V-P60R5 and V-P60R10 punches, respectively, in the order of 10 kN and 5 kN. In the previously conducted analysis, it was found that the V-P60R5 punch induced less springback and higher positive strain in the specimens. Ergo, a relationship can be established between the maximum load, springback, and strain: an increase in the maximum load applied to the specimens results in a higher positive strain, and consequently, reduced springback. More localized deformation in the specimen, in the contact zone between the punch and the sheet, leads to a high asymmetry between tension and compression deformations, causing less springback.

Finite element modelling

The simulation models in the Abaqus 2017 software were based on the experimental procedure conducted for the bending tests. The test piece was modelled with a total of 3200 linear hexahedral elements of type C3D8I, using a Structured meshing technique. The choice of the meshing element' geometry is due to the test piece's geometry since it has rectangular faces. To note, four layers of elements through the specimen thickness of the specimen was used. The dies and punches were modelled as analytical rigid 3D surfaces drawn with the respective bending angle, and bending radius, like in the experimental procedure. For the simulations, the material definition was carried out with the material's stress-strain curve, assuming the isotropic hardening. The initial yield locus shape is described by the Von Mises yield function.

The Abaqus 2017 simulations contained two models: one for simulating the bending test with tools and the specimen, and a second one solely responsible for simulating springback. To simulate bending, it was necessary to create a step and four boundary conditions. To streamline the simulation, the specimen was designed at only a quarter of its actual size, with two symmetry boundary conditions (along X and Z axes) assigned. The matrix was given a fixed boundary condition, and the punch had a linear and downward movement along the Y-axis. The displacement value for the corresponding bending test was determined experimentally. The algorithm used for contact interactions was the surface-to-surface type. After completing the simulation for bending, a model was created to simulate springback, which included all the information from the previous model except for the tools and their boundary conditions, as well as the interactions between the tool-specimen assembly. The bending step was replaced with the springback step, and a new boundary condition was introduced to fix the specimen. To maintain the information from the previous model, a Predefined Field was established.

The springback calculation was carried out in the same manner as the experimental procedure. Fig. 8 shows a comparison of the experimental results with those from simulations.

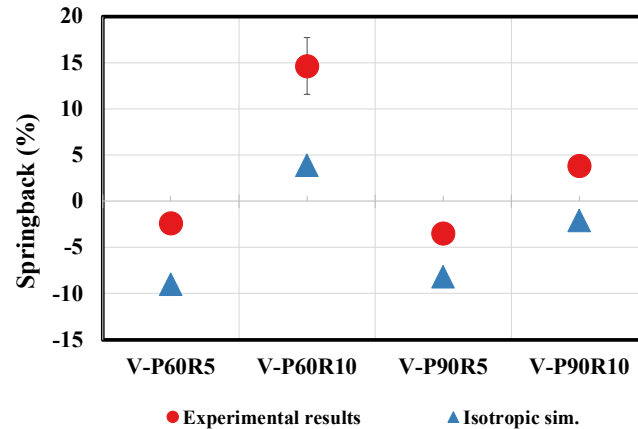


Fig. 8 - Springback results comparison between experimental and numerical results.

The occurrence of springback/forward is related to the punch radius in the experimental results, as mentioned earlier. Despite some variations between the experimental and numerical results, a consistent trend is observed, suggesting the presence of the punch geometry’s influence on the material’s springback in numerical simulations.

In the numerical simulations, the value of springback was higher for the radius 5 punches, which is contrary to what was observed in the experimental results. Among all the punches, the V-P60R5 punch caused the highest springback value at -8.98%, while the V-P90R10 punch showed the lowest at -2.08%. Except for the V-P60R10 punch, spring-forward was observed in all punches. However, this phenomenon may be related to the disparity between numerical and experimental results mentioned earlier. It is also noticeable that the springback value for the V-P60R10 punch shows the greatest deviation from the experimental value in the numerical simulations. An investigation was conducted to determine the cause of the deviation between experimental and numerical results. To test the influence of the friction coefficient value on the springback phenomenon, simulations were conducted with values of 0.05 and 0.15, in addition to the initial value of 0.1. However, the analysis showed that the difference in springback of the test specimen was negligible, so the value of 0.1 was retained. The steps' definition in the Abaqus 2017 software was also studied and it was concluded that changing the increment values (minimum, maximum, etc.) affects the springback of the test specimen, reducing it. Furthermore, modifying the boundary condition of the test specimen can also be explored to determine if it has any effect on the springback.

Besides springback analysis, the maximum load applied to each specimen in the numerical simulations was also studied. The charts were plotted with the Abaqus 2017’ data and are shown in Fig. 9 where a comparison can be seen between the numerical outcomes and the experimental results.

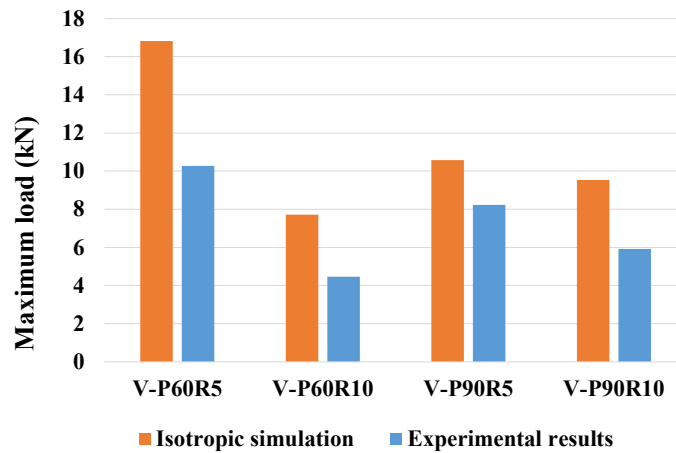


Fig. 9 - Comparison between the maximum load applied results of the Isotropic simulation and the experimental procedure.

It has been observed that there is a significant difference between the numerical and experimental outcomes, similar to the springback analysis. However, there is a noticeable pattern concerning the impact of the punch radius on springback, and its correlation with the maximum load. The test results indicate that 5 mm radius punches applied a higher maximum load on the samples, resulting in more springback than the 10 mm radius punches, which caused less springback. Hence, the numerical simulations were in line with the experimental results, as expected.

Conclusions

This study focuses on exploring the springback and spring-forward characteristics of third-generation steel, specifically USS CR980XG3™, through V-bending tests and numerical simulations. Four V-punches with varying bending angles and radii were used to conduct the tests. The study reveals that tool geometry has a significant impact on the springback of third-generation steel specimens during bending tests. The research also analyzes the effects of punch angle and radius on springback, strain, and maximum load. Experimental results show that a smaller punch radius leads to decreased springback due to more localized deformation in the contact zone between the punch top and the sheet. Furthermore, the experimental study indicates that the 60-degree punch induces higher springback than the 90-degree punch, though this difference is less pronounced with a 5 mm radius. The procedure has some limitations, such as reduced specimen thickness, which affects strain data capture by the Aramis system and may cause occasional inaccuracies.

Regarding the numerical study, the Abaqus 2017 software simulations were based on experimental bending tests, with careful consideration given to modelling parameters, meshing techniques, and material properties. Two distinct models were employed, one for simulating the bending test and another for assessing springback, each with specific boundary conditions and steps.

Despite observed some differences between numerical simulations and experimental results, a consistent trend emerged, highlighting the influence of punch geometry on material springback in the simulations. An investigation into the discrepancy of the results revealed negligible impact from variations in the friction coefficient, leading to the retention of the initial value of 0.1. Additionally, an exploration of step definitions in the Abaqus 2017 software indicated that modifying increment values and boundary conditions could potentially affect the springback phenomenon, providing avenues for further study.

In summary, while some differences persist between numerical simulations and experimental outcomes, this study sheds light on the significance of punch geometry in influencing material

springback. Further research into refining simulation parameters and boundary conditions may contribute to a more accurate representation of the observed phenomena in practical bending tests.

Acknowledgments

The authors acknowledge support from the Portuguese Foundation of Science and Technology (FCT), in its State Budget component (OE) through project 2022.05783.PTDC (<https://doi.org/10.54499/2022.05783.PTDC>). This article was also supported by the projects UIDB/00481/2020 and UIDP/00481/2020 - FCT, (<https://doi.org/10.54499/UIDB/00481/2020>) and (<https://doi.org/10.54499/UIDP/00481/2020>) and CENTRO-01-0145-FEDER-022083 Centro Portugal Regional Programme (Centro2020), under the PORTUGAL 2020 Partnership Agreement, through the European Regional Development Fund.

References

- [1] R.H. Wagoner, H. Lim, M.G. Lee, Advanced issues in springback, in: *Int J Plast*, Elsevier Ltd, 2013: pp. 3–20. <https://doi.org/10.1016/j.ijplas.2012.08.006>
- [2] D.K. Leu, Relationship between mechanical properties and geometric parameters to limitation condition of springback based on springback–radius concept in V-die bending process, *International Journal of Advanced Manufacturing Technology*. 101 (2019) 913–926. <https://doi.org/10.1007/s00170-018-2970-1>
- [3] W. Zhang, J. Xu, Advanced lightweight materials for Automobiles: A review, *Mater Des*. 221 (2022). <https://doi.org/10.1016/j.matdes.2022.110994>
- [4] S. 'Kalpakjian, S. 'Schmid, *Manufacturing Engineering & Technology*, 7th ed., Pearson Higher Education, 2013.
- [5] J.H. Schmitt, T. Iung, New developments of advanced high-strength steels for automotive applications, *C R Phys* 19 (2018) 641–656. <https://doi.org/10.1016/j.crhy.2018.11.004>
- [6] T.K. 'Roy, B. 'Bhattacharya, C. 'Ghosh, S.K.'Ajmani, *Advanced High Strength Steel: Processing and Applications*, Springer Singapore, 2018.
- [7] M.Y.'Demeri, *Advanced High-Strength Steels: Science, Technology, and Applications*, ASM International, 2013.
- [8] K. 'Lange, *Handbook of Metal Forming*, McGraw-Hill, 1985.
- [9] S. Thipprakmas, W. Phanitwong, Process parameter design of spring-back and spring-go in V-bending process using Taguchi technique, *Mater Des* 32 (2011) 4430–4436. <https://doi.org/10.1016/j.matdes.2011.03.069>
- [10] M. Özdemir, H. Gökmeşe, Microstructural characterization and deformation of X10CrAlSi24 sheet material applied V-bending process, *Tehnicki Vjesnik* 25 (2018) 846–854. <https://doi.org/10.17559/TV-20170425022545>
- [11] S. Thipprakmas, S. Rojananan, Investigation of spring-go phenomenon using finite element method, *Mater Des* 29 (2008) 1526–1532. <https://doi.org/10.1016/j.matdes.2008.02.002>.
- [12] H. Tschaetsch, *Metal Forming Practise*, Springer, 2006.
- [13] M. Wasif, A. Fatima, A. Ahmed, S.A. Iqbal, Investigation and Optimization of Parameters for the Reduced Springback in JSC-590 Sheet Metals Occurred During the V-Bending Process, *Transactions of the Indian Institute of Metals* 74 (2021) 2751–2760. <https://doi.org/10.1007/s12666-021-02357-9>

- [14] W. Lems, The change of Young's modulus of copper and silver after deformation at low temperature and its recovery, *Physica* 28 (1962) 445–452. [https://doi.org/10.1016/0031-8914\(62\)90022-8](https://doi.org/10.1016/0031-8914(62)90022-8)
- [15] R.M. Cleveland, A.K. Ghosh, Inelastic effects on springback in metals, *Int J Plast* 18 (2002) 769–785. [https://doi.org/10.1016/S0749-6419\(01\)00054-7](https://doi.org/10.1016/S0749-6419(01)00054-7)
- [16] Z.M. Fu, Numerical Simulation of Springback in Air-Bending Forming of Sheet Metal, *Applied Mechanics and Materials* 121–126 (2011) 3602–3606. <https://doi.org/10.4028/www.scientific.net/AMM.121-126.3602>.
- [17] D. Fei, P. Hodgson, Experimental and numerical studies of springback in air v-bending process for cold rolled TRIP steels, *Nuclear Engineering and Design* 236 (2006) 1847–1851. <https://doi.org/10.1016/j.nucengdes.2006.01.016>
- [18] M. Ramezani, Z.M. Ripin, A friction model for dry contacts during metal-forming processes, *The International Journal of Advanced Manufacturing Technology* 51 (2010) 93–102. <https://doi.org/10.1007/s00170-010-2608-4>
- [19] D.-K. Leu, Z.-W. Zhuang, Springback prediction of the vee bending process for high-strength steel sheets, *Journal of Mechanical Science and Technology* 30 (2016) 1077–1084. <https://doi.org/10.1007/s12206-016-0212-8>
- [20] M.L. Garcia-Romeu, J. Ciurana, I. Ferrer, Springback determination of sheet metals in an air bending process based on an experimental work, *J Mater Process Technol* 191 (2007) 174–177. <https://doi.org/10.1016/j.jmatprotec.2007.03.019>
- [21] R.O. Santos, L.P. Moreira, M.C. Butuc, G. Vincze, A.B. Pereira, Damage Analysis of Third-Generation Advanced High-Strength Steel Based on the Gurson–Tvergaard–Needleman (GTN) Model, *Metals (Basel)* 12 (2022) 214. <https://doi.org/10.3390/met12020214>
- [22] Ö. Tekaslan, N. Gerger, U. Şeker, Determination of spring-back of stainless steel sheet metal in “V” bending dies, *Mater Des* 29 (2008) 1043–1050. <https://doi.org/10.1016/j.matdes.2007.04.004>
- [23] Springback/Springforward Behaviour of DP Steels Used in the Automotive Industry, *Tehnicki Vjesnik - Technical Gazette* 27 (2020). <https://doi.org/10.17559/TV-20181004144024>
- [24] M.L. Garcia-Romeu, J. Ciurana, I. Ferrer, Springback determination of sheet metals in an air bending process based on an experimental work, *J Mater Process Technol* 191 (2007) 174–177. <https://doi.org/10.1016/j.jmatprotec.2007.03.019>